Composites Communications 30 (2022) 101053

Contents lists available at ScienceDirect

Composites Communications

journal homepage: www.elsevier.com/locate/coco

Organo-functionalized MoS_2 as a nanofiller to enhance and control the swelling behavior of polybutadiene rubber nanocomposites

Rodrigo Fiel [a,*], Ingrid D. Barcelos [b], Edson Roberto Leite [a,c,**]

[a] Chemistry Department, Federal University of Sao Carlos, Sao Paulo, Brazil
[b] Brazilian Synchrotron Light Laboratory (LNLS), Brazilian Center for Research in Energy and Materials (CNPEM), Zip Code 13083-970, Campinas, Sao Paulo, Brazil
[c] Brazilian Nanotechnology National Laboratory (LNNano), Brazilian Center for Research in Energy and Materials (CNPEM), Campinas SP, Brazil

ARTICLE INFO

Keywords:
MoS_2 functionalization
Rubber nanocomposites
Swelling behavior

ABSTRACT

The functionalized MoS_2 (f-MoS_2), synthesized at different temperatures, was incorporated in polybutadiene (PB) rubber as a nanofiller and then vulcanized with sulfur without any further additives. The incorporation of f-MoS_2 into PB matrix promotes significant improvements in swelling properties that can be even compared to traditional fluorocarbon (FKM) and nitrile (NBR) rubbers. Moreover, the statistical results showcase that is possible to modulate the swelling behavior of the rubber nanocomposite by varying the amount of PB grafted on f-MoS_2.

1. Introduction

High-performance rubber nanocomposites have attracted attention owing to their wide range of applications which combines the viscoelastic properties of rubbers with the functionality of several types of reinforcing nanofillers [1–7]. Currently, the research on developing novel nanofillers becomes imperative in order to enhance the thermal, mechanical, swelling and processing properties as well as to overcome the environmental drawbacks caused by carbon black, which is the most used filler in the rubber industry [8].

Over the years, two-dimensional MoS_2 has emerged as a potential nanofiller candidate to be incorporated in rubbers [9] because of its high Young's modulus (0.3 TPa) [10] allied with fascinating properties in catalysis [11], sensors [12,13], and field-effect transistors [14,15]. However, a homogeneous dispersion of MoS_2 in polymeric matrices cannot be easily achieved using traditional blending techniques due to the lack of reactive groups and poor interaction with solvents of most of polymer matrices [16]. A further step towards enhancing the MoS_2 dispersion is by surface functionalization with covalent or non-covalent ligands [17,18]. For instance, recent advances have been reported on MoS_2 functionalized with organic thiol ligands (non-covalent) [19], diazonium salts (covalent) [20], and different polymers (covalent/non-covalent) [21]. Typically, rubbers are cross-linked polymers able to absorb a large amount of solvent without dissolving [22] and the incorporation of functionalized MoS_2 in these types of polymers represents a growing field of applications due to the excellent swelling control and enhanced mechanical properties [23,24]. In this context, polybutadiene (PB) rubber, an example of cross-linked polymer [25,26], is an interesting prototype to investigate the effects induced by functionalized MoS_2 on its structure. PB is present as a copolymer with nitrile or styrene resulting, respectively, in nitrile-butadiene rubber (NBR) and styrene-butadiene rubber (SBR), which are the most important commercial rubbers due to its widespread industrial applications [27]. The investigation of swelling-ratio on novel rubbers nanocomposites is essential to determine its structure [28] and potential industrial applications (*i.e.* automotive, aerospace, oil and gas, etc.) [29]. Apart from fluorocarbon rubber (FKM), which exhibits outstanding chemical resistance, traditional rubbers (i.e. PB, SBR and NBR) are usually nonresistant to organic solvents, certain types of oils and greases which impair their properties and the effects are undesirable in most applications. However, as it is known, the fabrication of FKM is difficult and expensive, leading to the development of new functional rubbers with high chemical resistance (low swelling-ratio) for advanced applications [30,31].

In this communication, MoS_2 was functionalized with PB (f-MoS_2) via single-step liquid-phase exfoliation (LPE) process using ultrasonic bath at different temperatures following the protocol that we previously reported [32]. Here, we noticed that is possible to control the concentration of PB grafted on the edge sites of MoS_2 by controlling the ultrasound bath temperature. Moreover, the f-MoS_2s nanofiller were

* Corresponding author.
** Corresponding author. Chemistry Department, Federal University of Sao Carlos, Sao Paulo, Brazil.
E-mail addresses: rodrigospfiel@gmail.com (R. Fiel), edson.leite@lnnano.cnpem.br (E.R. Leite).

https://doi.org/10.1016/j.coco.2021.101053
Received 1 September 2021; Received in revised form 1 December 2021; Accepted 23 December 2021
Available online 8 January 2022

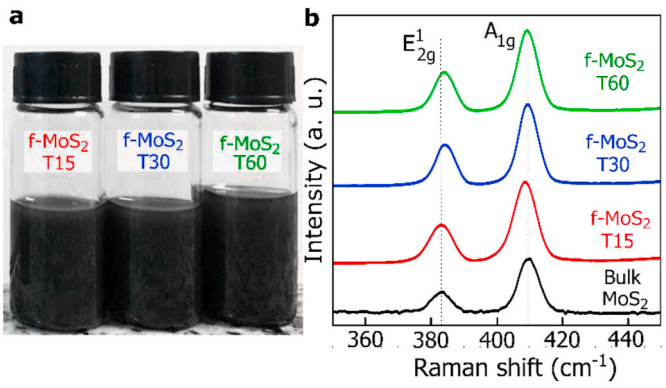

Fig. 1. a) Photograph of f-MoS_2 colloidal dispersions in toluene: f-MoS_2T15, f-MoS_2T30 and f-MoS_2T60. b) Raman spectra of bulk-MoS_2 (black), f-MoS_2T15 (red), f-MoS_2T30 (blue) and f-MoS_2T60 (green). (For interpretation of the references to colour in this figure legend, the reader is referred to the Web version of this article.)

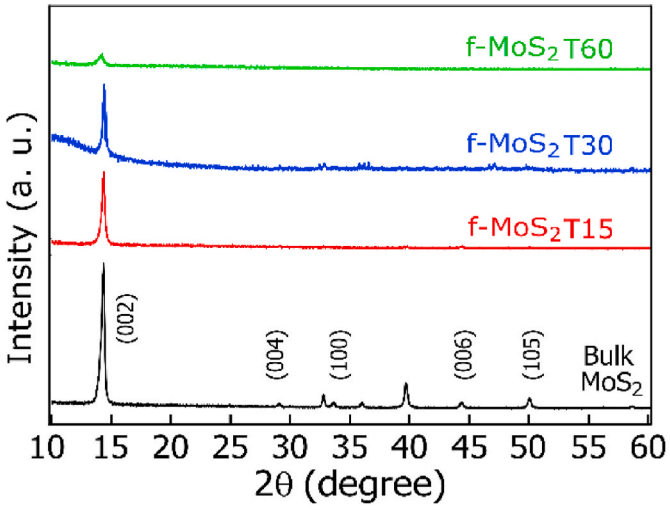

Fig. 2. XRD diffractogram of bulk-MoS_2 (black) and the respective f-MoS_2: f-MoS_2T15 (red), f-MoS_2T30 (blue), and f-MoS_2T60 (green). (For interpretation of the references to colour in this figure legend, the reader is referred to the Web version of this article.)

incorporated in different loadings in PB and then vulcanized only with sulfur, without any further additives, resulting in f-MoS_2/PB rubber nanocomposites that showed significant improvements on the reduction of swelling ratio compared to neat PB and traditional commercial rubbers (i.e. FKM and NBR) in toluene and methyl-ethyl ketone (MEK). The results indicated that the swelling behavior of the f-MoS_2/PB is governed by the amount of PB functionalized onto MoS_2 surface. Our findings provide new insights into improving swelling control in rubber induced by functionalized layered materials without using carbon black in its composition.

2. Results and discussion

We start the discussion by performing the morphological and structural characterization of the materials obtained. Fig. 1a shows that f-MoS_2 synthesized at 15 °C (f-MoS_2T15), 30 °C (f-MoS_2T30) and 60 °C (f-MoS_2T60) have high colloidal stability after six days in the ultrasonic bath (See Materials and Methods in SI). It is expected that the temperature plays an important role in LPE methods [33,34], inducing modification of the materials properties and solution concentration [35]. Fig. 1b shows the Raman spectra collected for bulk MoS_2 and f-MoS_2s. The frequency difference between E^1_{2g} and A_{1g} is 26.5 cm^{-1} for bulk--MoS_2, as expected for non-exfoliated material [36]. For f-MoS_2s, the frequency difference ranged from 24.8 to 25.5 cm^{-1}, indicating a high degree of exfoliation (~4–10 layers) [37]. Note that the frequency difference decreases when f-MoS_2 is synthesized at higher temperatures (i.e. f-MoS_2T60), corroborating to the fact that the higher the temperature during the LPE process, the thinner are the exfoliated flakes obtained [33,34]. This is also in agreement with our AFM analysis. The line profile analysis obtained by AFM shows f-MoS_2 sheets ranging from ~5.5 nm (f-MoS_2T60) to ~7.0 nm (f-MoS_2T15) of height, which is equivalent to 7–9 layers [38] (See Figure S1a-c, SI). Furthermore, UV–visible spectra (Figs. S2 and SI) show the characteristics A and B excitonic absorption bands at 612 nm and 674 nm, respectively, which also indicates the exfoliation of MoS_2 [39].

The diffractogram of bulk MoS_2 in Fig. 2 showed all characteristic peaks expected for this material corresponding (002), (004), (100), (103), (006), and (105) planes. The diffractogram of f-MoS_2 showed the absence of all peaks except the peak corresponding to the basal plane (002) that indicates the exfoliation of the sheets. The presence of only (002) plane suggests restacking of the functionalized sheets on the substrate during the drying process. The restacking has been reported in several works, mainly in the process involving lithium intercalation [40]. SEM images reveal that f-MoS_2s are morphologically different from the bulk MoS_2 [41] (See Figure S3-S5, SI) and the functionalized nanosheets are randomly oriented. In addition, it is possible to verify the random stacking corroborating with the diffraction patterns in Fig. 2 [42]. AFM and SEM images also show flakes with a lateral size smaller than 1.0 μm and few surface defects.

The electronic structure and the interaction between MoS_2 and PB chains were studied by TEM and XPS. The representative TEM image (See Figure S6a-c, SI) shows several f-MoS_2 flakes electron transparent indicating a high degree of exfoliation which agrees with Raman measurements. After the deconvolution process, the XPS spectra of Mo3d show the 226.2eV peak referring to the S2s of S^{-2}, 229.4eV and 232.6eV peaks corresponding to Mo–S bonds of Mo^{4+} $3d_{5/2}$ and Mo^{4+} $3d_{3/2}$, respectively [43]. Furthermore, it was able to identify the 233.7eV and 236.2eV corresponding to Mo–O bonds of Mo^{6+} $3d_{5/2}$ e $Mo^{6+}3d_{3/2}$, respectively [43]. The partial oxidation of MoS_2 is due to the oxidative mechanism in LPE process [35] (See Figs. S7a–c). Next, to verify the chemical interaction between PB and MoS_2 flakes, carbon C1s peaks were evaluated (Figs. S8a–c). The analysis of C1s peaks of neat PB showed C═C, C–C, and C–H bonds as expected. However, the analysis of f-MoS_2s showed a complex set of C1s peaks after the deconvolution process. We identified peaks at 286.6eV and 288.7eV, indicating C–C–S and C–S bonds, respectively, regardless of the synthesis temperature [44]. The sulfur S2p of f-MoS_2 also suggests the presence of S–C peaks at 164.8eV (See Figs. S9a–c) [45]. Therefore, our analysis suggests that the functionalization occurs regardless of synthesis temperature.

Thermogravimetric analysis (TGA) (Figs. S10 and SI) was performed in order to quantify the amount of PB present in f-MoS_2s as well as to verify its correlation with the ultrasound bath temperature of the single-step LPE method. Bulk MoS_2 undergoes a thermal degradation at 377 °C with a weight loss of 12.68 wt% that we attribute to the loss of SO_2 during this thermal event [46]. The difference between the bulk MoS_2 curve and f-MoS_2s represents, exclusively, the mass loss of the PB grafted on the MoS_2. Thus, TGA curves indicated a PB concentration of 2.57 wt %, 6.68 wt%, and 7.60 wt% for f-MoS_2T15, f-MoS_2T30 and f-MoS_2T60, respectively. The increase in PB concentration on MoS_2 (almost three-fold between 60 °C and 15 °C) may be due to cascade effects: initially, increasing temperature increases the sonication induced scission events. Then, the successive scissions in ultrasound bath leads to an increasing number of sulfur active edge sites of MoS_2 that interact with more PB chains [35,40]. Now, we focus our attention to the swelling behavior of f-MoS_2/PB rubber nanocomposites (Figure S11a-j, SI). The swelling ratio depends on the nature of the additives, their

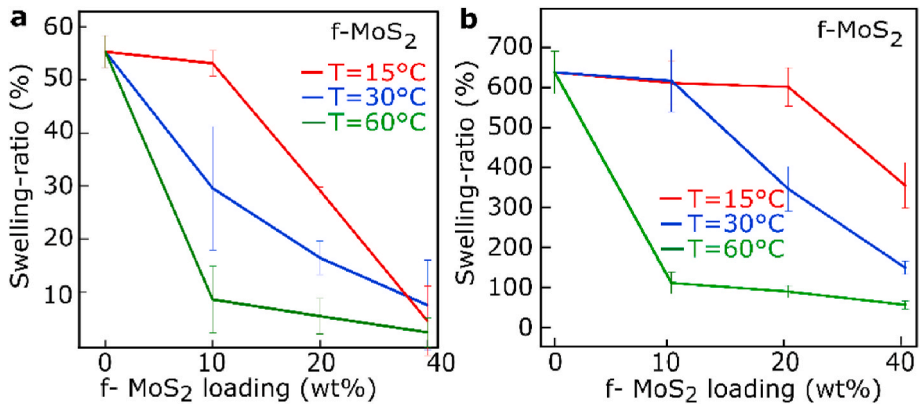

Fig. 3. Swelling-ratio curves of neat PB and f-MoS_2/PB rubber nanocomposites as a function of nanofiller loading and its synthesis temperature: a) in MEK and b) in toluene.

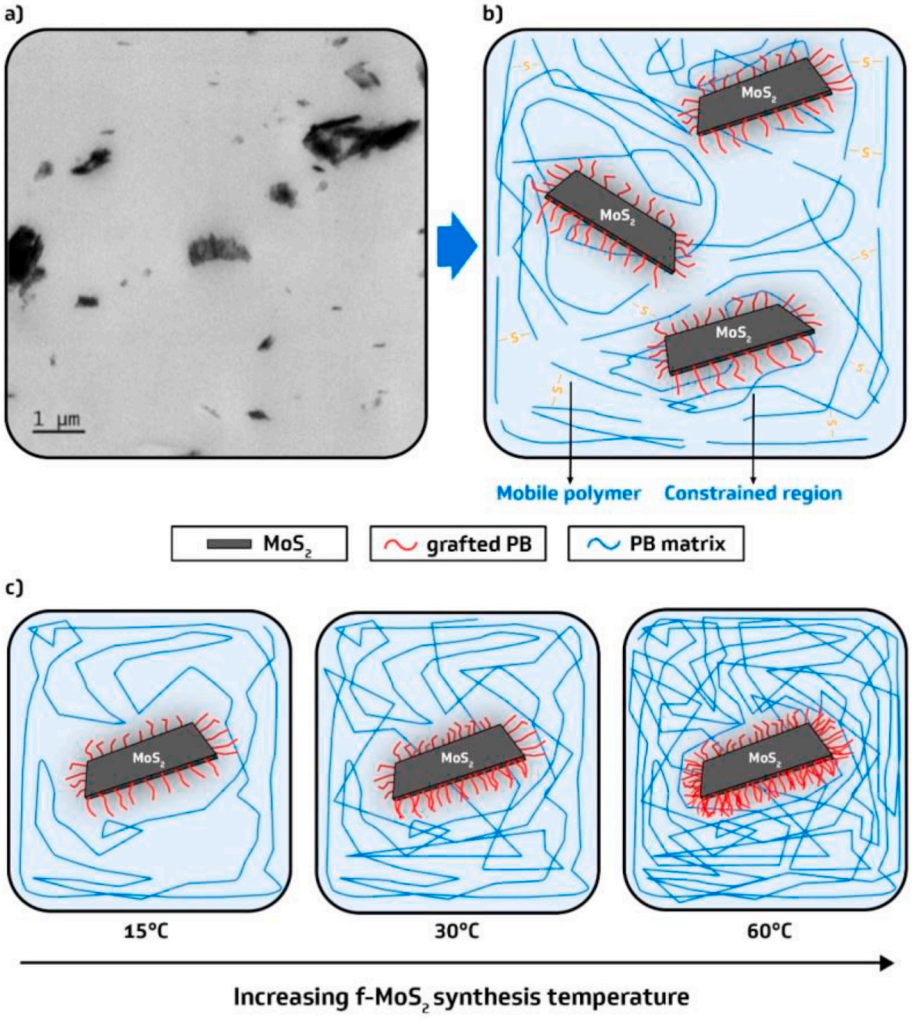

Fig. 4. a) TEM image of f-MoS_2T60/PB rubber at 40 wt%. Schematic illustrations of f-MoS_2/PB nanocomposites: b) proposed interaction between PB matrix and f-MoS_2 and c) proposed interaction between PB matrix and f-MoS_2 synthesized under different ultrasound bath temperatures.

concentration/dispersion and processing [47]. Fig. 3a–b shows the swelling behavior of neat PB and f-MoS_2/PB rubber nanocomposites in MEK and toluene, as a function of the f-MoS_2 loading (wt%) and its synthesis temperature.

One can see that for all samples there is a significant reduction on the swelling ratio with increasing the f-MoS_2 loading or its synthesis temperature (See Table S1 in SI). For instance, the f-MoS_2T60/PB 40 wt % rubber nanocomposite, which presented the best result, swelled 3.26 ± 2.72% in MEK (Figs. 3a) and 55.00 ± 10.00% in toluene (Fig. 3b). The swelling of neat PB rubber was 56.22 ± 3.00% in MEK (the first measurement is shown in Fig. 3a) and 637.00 ± 53.00% in toluene (the first measurement is shown in Fig. 3b), respectively. The comparative

swelling test for NBR and FKM in MEK were 122.00 ± 0.04% and 168.00 ± 0.03%, respectively. In toluene, the swelling ratio for NBR and MEK were 61.00 ± 0.007% and 8.00 ± 0.028%, respectively. Note that even neat PB rubber had better swelling performance in MEK than NBR and FKM. This result may be ascribed to the polarity difference between MEK and PB: particularly, MEK is considered a polar solvent due to ketone function in its structure. On the other hand, PB is highly non-polar rubber which hinders the rubber/solvent interaction. Both NBR and FKM have polar groups in its structure (i.e. acrylonitrile and fluorine) which facilitates the rubber/solvent interaction leading to higher swelling-ratio. TEM image (Fig. 4a) revealed a good compatibility and dispersion, even at 40 wt%, between f-MoS_2 nanofiller and PB matrix without signs of percolation. Therefore, the striking reduction in swelling ratio of the rubber nanocomposites must be a direct consequence of interfacial nanofiller/PB interaction in such a way that the swelling results can be compared to swelling of traditional FKM and NBR rubbers. Obviously, FKM presented a lower swelling ratio in toluene compared to f-MoS_2T60/PB 40 wt% rubber nanocomposite. However, it is worth remembering that both FKM and NBR have several additives in its formulation, such as, zinc oxide, oils, plasticizers and, of course, carbon black (See rubber formulations in Tables S2 and S3, SI). Those additives were not used in this study in order to evaluate the effect of the nanofillers and its loadings on swelling behavior of rubber nanocomposites. Based on these results, we believe that the grafted PB, induced by MoS_2, is acting as a cross-linking agent in the PB matrix that contributes for the great reduction on swelling ratio by reducing the free volume of PB rubber structure [48] (Fig. 4b). The reduction of free volume in rubber structure creates constrained regions [49] that hampers the penetration of the solvent in the polymeric matrix [50].

Through statistical analysis (See Tables S4 and S5 and statistical discussion in SI), our results in Fig. 3a–b indicate that the swelling properties of rubber nanocomposites depend on the nanofiller loading and its synthesis temperature. Clearly, it is expected a reduction on swelling ratio as nanofiller loading increase because the interactions between nanofiller/PB will increase, reducing the free volume. According to swelling ratio curves in Fig. 3a–b and the data in Table S1 (See SI), as the f-MoS_2 synthesis temperature increase, at constant nanofiller loading, we noticed a reduction of the swelling ratio of the rubber nanocomposites. In this case, we believe that the effect of synthesis temperature on swelling behavior is intimately correlated with LPE exfoliation mechanism [35,40] which increases the amount of PB functionalized on the edge sites of f-MoS_2 calculated by TGA. Therefore, increasing the grafted PB concentration will interact more efficiently with PB matrix creating more constrained regions compared to the same f-MoS_2 synthesized at lower temperatures (Fig. 4c).

3. Conclusion

In summary, functionalized f-MoS_2 nanofillers were synthesized through single-step LPE at different ultrasound bath temperatures. The incorporation of f-MoS_2 in PB rubber without any further additives promoted significant enhancement on swelling properties that can be compared to traditional commercial rubbers (namely FKM and NBR). This is an interesting result that turns f-MoS_2 nanofiller as a great candidate to replace carbon black in rubber formulations. Moreover, through statistical analysis (See SI), we noticed a direct and independent correlation between the synthesis temperature of nanofiller and its loading in a PB matrix on the reduction of the swelling ratio. Thus, we were able to modulate the amount of absorbed solvent with nanofiller loading or its temperature of synthesis. Finally, the results showed that the enhancement on swelling property is due to the good interface interaction between grafted PB in f-MoS_2 and PB matrix reducing the free volume in rubber nanocomposite structure. The f-MoS_2 nanofiller opens new opportunities for the development of novel and functionalized materials with superior swelling characteristics and controlled chemical resistance.

CRediT authorship contribution statement

Rodrigo Fiel: Conceptualization, Methodology, Investigation, Writing – original draft, Investigation, Data curation, Validation. **Ingrid D. Barcelos:** Writing – review & editing, Visualization, Supervision, Formal analysis. **Edson Roberto Leite:** Supervision, Project administration.

Declaration of competing interest

The authors declare that they have no known competing financial interests or personal relationships that could have appeared to influence the work reported in this paper.

Acknowledgements

This work was supported by FAPESP (Proc. 2016/20493-0) and FAPESP CEPID CDMF (Proc. 13/07296–2). CAPES and CNPq are gratefully acknowledged. R.F. acknowledges Prof. Edenir R.P. Filho for contributions on statistical discussion. I.D.B. acknowledges the financial support from the Brazilian Nanocarbon Institute of Science and Technology (INCT/Nanocarbono) and the support from CNPq through the research grant 311327/2020-6. The authors acknowledge ME laboratory of LNNano for the use of electron microscopy facility.

Appendix A. Supplementary data

Supplementary data to this article can be found online at https://doi.org/10.1016/j.coco.2021.101053.

References

[1] A. Sinclair, X. Zhou, S. Tangpong, D.S. Bajwa, M. Quadir, L. Jiang, High-performance styrene-butadiene rubber nanocomposites reinforced by surface-modified cellulose nanofibers, ACS Omega 4 (2019) 13189–13199, https://doi.org/10.1021/acsomega.9b01313.

[2] L. Cao, Z. Gong, C. Xu, Y. Chen, Mechanical strong and recyclable rubber nanocomposites with sustainable cellulose nanocrystals and interfacial exchangeable bonds, ACS Sustain. Chem. Eng. (2021), https://doi.org/10.1021/acssuschemeng.1c02581.

[3] X. Wang, J. Qiao, Z. Zhou, J. Gao, G. Qi, B. Li, J. Zhang, X. Zhang, Elastomeric nanoparticles: effective additive for high performance rubber nanocomposites, Rubber Chem. Technol. 93 (2020) 445–456, https://doi.org/10.5254/rct.20.80366.

[4] H. Shimamoto, C.-H. Cheng, K. Kamitani, K. Kojio, Y. Higaki, A. Takahara, Nanocomposite elastomers composed of silica nanoparticles grafted with a comb-shaped copolymer brush, Macromolecules 52 (2019) 5963–5970, https://doi.org/10.1021/acs.macromol.9b00927.

[5] Y. Su, H. Che, Z. Zhang, S. Zeng, Y. Xu, W. Nie, Y. Zhou, P. Chen, Interface optimization of silicone rubber/molybdenum disulfide composites for enhanced mechanical and thermal properties, Compos. Commun. 28 (2021) 100900, https://doi.org/10.1016/j.coco.2021.100900.

[6] J. Zhao, J. Zhang, L. Wang, J. Li, T. Feng, J. Fan, L. Chen, J. Gu, Superior wave-absorbing performances of silicone rubber composites via introducing covalently bonded SnO2@MWCNT absorbent with encapsulation structure, Compos. Commun. 22 (2020) 100486, https://doi.org/10.1016/j.coco.2020.100486.

[7] Q. Tian, Y. Tang, T. Ding, X. Li, Z. Zhang, Effect of nano-silica surface-capped by bis [3-(triethoxysilyl)propyl] tetrasulfide on the mechanical properties of styrene-butadiene rubber/butadiene rubber nanocomposites, Compos. Commun. 10 (2018) 190–193, https://doi.org/10.1016/j.coco.2018.10.005.

[8] M. Arroyo, M.A. López-Manchado, B. Herrero, Organo-montmorillonite as substitute of carbon black in natural rubber compounds, Polymer 44 (2003) 2447–2453, https://doi.org/10.1016/S0032-3861(03)00090-9.

[9] B. Améduri, B. Boutevin, G. Kostov, Fluoroelastomers: synthesis, properties and applications, Prog. Polym. Sci. 26 (2001) 105–187, https://doi.org/10.1016/S0079-6700(00)00044-7.

[10] A. Castellanos-Gomez, M. Poot, G.A. Steele, H.S.J. van der Zant, N. Agraït, G. Rubio-Bollinger, Elastic properties of freely suspended MoS2 nanosheets, Adv. Mater. 24 (2012) 772–775, https://doi.org/10.1002/adma.201103965.

[11] G. Li, Z. Chen, Y. Li, D. Zhang, W. Yang, Y. Liu, L. Cao, Engineering substrate interaction to improve hydrogen evolution catalysis of monolayer MoS2 films beyond Pt, ACS Nano 14 (2020) 1707–1714, https://doi.org/10.1021/acsnano.9b07324.

[12] N.P. Rezende, A.R. Cadore, A.C. Gadelha, C.L. Pereira, V. Ornelas, K. Watanabe, T. Taniguchi, A.S. Ferlauto, A. Malachias, L.C. Campos, R.G. Lacerda, Probing the electronic properties of monolayer MoS2 via interaction with molecular hydrogen,

Adv. Electron. Mater. 5 (2019) 1800591, https://doi.org/10.1002/aelm.201800591.
[13] A. Ayari, E. Cobas, O. Ogundadegbe, M.S. Fuhrer, Realization and electrical characterization of ultrathin crystals of layered transition-metal dichalcogenides, J. Appl. Phys. 101 (2007), 014507, https://doi.org/10.1063/1.2407388.
[14] B. Radisavljevic, A. Radenovic, J. Brivio, V. Giacometti, A. Kis, Single-layer MoS2 transistors, Nat. Nanotechnol. 6 (2011) 147–150, https://doi.org/10.1038/nnano.2010.279.
[15] G. Guan, M.Y. Han, Functionalized hybridization of 2D nanomaterials, Adv. Sci. 6 (2019), https://doi.org/10.1002/advs.201901837.
[16] C.L.C. Rodriguez, M.A.B.S. Nunes, P.S. Garcia, G.J.M. Fechine, Molybdenum disulfide as a filler for a polymeric matrix at an ultralow content: polystyrene case, Polym. Test. 93 (2021) 106882, https://doi.org/10.1016/j.polymertesting.2020.106882.
[17] S. Presolski, M. Pumera, Covalent functionalization of MoS2, mater, Today 19 (2016) 140–145, https://doi.org/10.1016/j.mattod.2015.08.019.
[18] I.K. Sideri, R. Arenal, N. Tagmatarchis, Covalently functionalized MoS2 with dithiolenes, ACS Mater. Lett. 2 (2020) 832–837, https://doi.org/10.1021/acsmaterialslett.0c00108.
[19] D. Voiry, A. Goswami, R. Kappera, C. de C.C. e Silva, D. Kaplan, T. Fujita, M. Chen, T. Asefa, M. Chhowalla, Covalent functionalization of monolayered transition metal dichalcogenides by phase engineering, Nat. Chem. 7 (2015) 45–49, https://doi.org/10.1038/nchem.2108.
[20] Q.-Q. Fu, Y.-D. Li, H.-H. Li, L. Xu, Z.-H. Wang, S.-H. Yu, In situ seed-mediated high-yield synthesis of copper nanowires on large scale, Langmuir 35 (2019) 4364–4369, https://doi.org/10.1021/acs.langmuir.9b00042.
[21] Z. Cheng, B. He, L. Zhou, A general one-step approach for in situ decoration of MoS2 nanosheets with inorganic nanoparticles, J. Mater. Chem. A. 3 (2015) 1042–1048, https://doi.org/10.1039/C4TA04946B.
[22] M. Bhattacharya, A.K. Bhowmick, Polymer–filler interaction in nanocomposites: new interface area function to investigate swelling behavior and Young's modulus, Polymer 49 (2008) 4808–4818, https://doi.org/10.1016/j.polymer.2008.09.002.
[23] L. Ries, E. Petit, T. Michel, C.C. Diogo, C. Gervais, C. Salameh, M. Bechelany, S. Balme, P. Miele, N. Onofrio, D. Voiry, Enhanced sieving from exfoliated MoS2 membranes via covalent functionalization, Nat. Mater. 18 (2019) 1112–1117, https://doi.org/10.1038/s41563-019-0464-7.
[24] K.M. Lee, Y. Oh, H. Yoon, M. Chang, H. Kim, Multifunctional role of MoS2 in preparation of composite hydrogels: radical initiation and cross-linking, ACS Appl. Mater. Interfaces 12 (2020) 8642–8649, https://doi.org/10.1021/acsami.9b19567.
[25] R.R. S, A.K. Bhowmick, S.K. De, S. Bandyopadhyay, Short melamine fiber filled nitrile rubber composites, J. Appl. Polym. Sci. 90 (2003) 544–558, https://doi.org/10.1002/app.12709.
[26] L.U. Devi, S.S. Bhagawan, S. Thomas, Mechanical properties of pineapple leaf fiber-reinforced polyester composites, J. Appl. Polym. Sci. 64 (1997) 1739–1748.
[27] Rubber chemistry, by J. Brydson, applied science publishers, London, 1978, 462 pp. Price: $64.00 T.F. Reed, J. Polym. Sci. Polym. Lett. Ed. 20 (1982) 202–203, https://doi.org/10.1002/pol.1982.130200316.
[28] S.C. George, M. knörgen, S. Thomas, Effect of nature and extent of crosslinking on swelling and mechanical behavior of styrene–butadiene rubber membranes, J. Membr. Sci. 163 (1999) 1–17, https://doi.org/10.1016/S0376-7388(99)00098-8.
[29] M. Abu-Abdeen, I. Elamer, Mechanical and swelling properties of thermoplastic elastomer blends, Mater. Des. 31 (2010) 808–815, https://doi.org/10.1016/j.matdes.2009.07.059.
[30] T. Brändel, M. Dirksen, T. Hellweg, Tuning the swelling properties of smart multiresponsive core-shell microgels by copolymerization, Polymers 11 (2019) 1269, https://doi.org/10.3390/polym11081269.
[31] S.F. Anis, R. Hashaikeh, N. Hilal, Functional materials in desalination: a review, Desalination (2019) 468, https://doi.org/10.1016/j.desal.2019.114077.
[32] R.H. Gonçalves, R. Fiel, M.R.S. Soares, W.H. Schreiner, C.M.P. Silva, E.R. Leite, Single-step exfoliation and covalent functionalization of MoS2 nanosheets by an organosulfur reaction, Chem. Eur J. 21 (2015) 15583–15588, https://doi.org/10.1002/chem.201502303.
[33] Y.-T. Liu, X.-D. Zhu, X.-M. Xie, Direct exfoliation of high-quality, atomically thin MoSe2 layers in water, Adv. Sustain. Syst. 2 (2018) 1700107, https://doi.org/10.1002/adsu.201700107.
[34] Y. Xu, H. Cao, Y. Xue, B. Li, W. Cai, Liquid-phase exfoliation of graphene: an overview on exfoliation media, techniques, and challenges, Nanomaterials 8 (2018), https://doi.org/10.3390/nano8110942.
[35] A. Jawaid, D. Nepal, K. Park, M. Jespersen, A. Qualley, P. Mirau, L.F. Drummy, R. A. Vaia, Mechanism for liquid phase exfoliation of MoS2, Chem. Mater. 28 (2016) 337–348, https://doi.org/10.1021/acs.chemmater.5b04224.
[36] H. Li, Q. Zhang, C.C.R. Yap, B.K. Tay, T.H.T. Edwin, A. Olivier, D. Baillargeat, From bulk to monolayer MoS2: evolution of Raman scattering, Adv. Funct. Mater. 22 (2012) 1385–1390, https://doi.org/10.1002/adfm.201102111.
[37] Y. Lee, S. Bae, H. Jang, S. Jang, S.-E. Zhu, S.H. Sim, Y. Il Song, B.H. Hong, J.-H. Ahn, Wafer-scale synthesis and transfer of graphene films, Nano Lett. 10 (2010) 490–493, https://doi.org/10.1021/nl903272n.
[38] H. Terrones, E. Del Corro, S. Feng, J.M. Poumirol, D. Rhodes, D. Smirnov, N. R. Pradhan, Z. Lin, M.A.T. Nguyen, A.L. Elías, T.E. Mallouk, L. Balicas, M. A. Pimenta, M. Terrones, New first order Raman-active modes in few layered transition metal dichalcogenides, Sci. Rep. 4 (2014) 4215, https://doi.org/10.1038/srep04215.
[39] A. Splendiani, L. Sun, Y. Zhang, T. Li, J. Kim, C.-Y. Chim, G. Galli, F. Wang, Emerging photoluminescence in monolayer MoS2, Nano Lett. 10 (2010) 1271–1275, https://doi.org/10.1021/nl903868w.
[40] J. Heising, M.G. Kanatzidis, Structure of restacked MoS2 and WS2 elucidated by electron crystallography, J. Am. Chem. Soc. 121 (1999) 638–643, https://doi.org/10.1021/ja983043c.
[41] W. Zhang, X. Xiao, Y. Li, X. Zeng, L. Zheng, C. Wan, Liquid-exfoliation of layered MoS2 for enhancing photocatalytic activity of TiO2/g-C3N4 photocatalyst and DFT study, Appl. Surf. Sci. 389 (2016) 496–506, https://doi.org/10.1016/j.apsusc.2016.07.154.
[42] X. Qian, K. Xie, S. Guo, Q. Liang, S. Zhang, Z. Xiong, H. Zhan, C. Liu, X. Yang, J. Zhu, D. Li, Beneficial restacking of 2D nanomaterials for electrocatalysis: a case of MoS2 membranes, Chem. Commun. 56 (2020) 7005–7008, https://doi.org/10.1039/D0CC02139C.
[43] A. Santoni, F. Rondino, C. Malerba, M. Valentini, A. Mittiga, Electronic structure of Ar + ion-sputtered thin-film MoS 2 : a XPS and IPES study, Appl. Surf. Sci. 392 (2017) 795–800, https://doi.org/10.1016/j.apsusc.2016.09.007.
[44] H. Yu, Y. Jin, Z. Li, F. Peng, H. Wang, Synthesis and characterization of sulfonated single-walled carbon nanotubes and their performance as solid acid catalyst, J. Solid State Chem. 181 (2008) 432–438, https://doi.org/10.1016/j.jssc.2007.12.017.
[45] J. Ye, F. He, J. Nie, Y. Cao, H. Yang, X. Ai, Sulfur/carbon nanocomposite-filled polyacrylonitrile nanofibers as a long life and high capacity cathode for lithium–sulfur batteries, J. Mater. Chem. A. 3 (2015) 7406–7412, https://doi.org/10.1039/C4TA06976E.
[46] N. Wakabayashi, H.G. Smith, R.M. Nicklow, Lattice dynamics of hexagonal Mo ${\mathrm{S}}_{2}$ studied by neutron scattering, Phys. Rev. B 12 (1975) 659–663, https://doi.org/10.1103/PhysRevB.12.659.
[47] Z. Bartczak, A.S. Argon, R.E. Cohen, M. Weinberg, Toughness mechanism in semi-crystalline polymer blends: II. High-density polyethylene toughened with calcium carbonate filler particles, Polymer 40 (1999) 2347–2365, https://doi.org/10.1016/S0032-3861(98)00444-3.
[48] L. Bokobza, The reinforcement of elastomeric networks by fillers, Macromol. Mater. Eng. 289 (2004) 607–621, https://doi.org/10.1002/mame.200400034.
[49] Y. Lin, S. Liu, J. Peng, L. Liu, The filler–rubber interface and reinforcement in styrene butadiene rubber composites with graphene/silica hybrids: a quantitative correlation with the constrained region, Compos. Part A Appl. Sci. Manuf. 86 (2016) 19–30, https://doi.org/10.1016/j.compositesa.2016.03.029.
[50] W. Hirunpinyopas, E. Prestat, S.D. Worrall, S.J. Haigh, R.A.W. Dryfe, M.A. Bissett, Desalination and nanofiltration through functionalized laminar MoS2 membranes, ACS Nano 11 (2017) 11082–11090, https://doi.org/10.1021/acsnano.7b05124.